Dynamic Jahn-Teller viewpoint for generation mechanism of asymmetric modes of coherent phonons

Yosuke Kayanuma and Kazutaka G. Nakamura

Phys. Rev. B **95**, 104302 — Published 8 March 2017

DOI: 10.1103/PhysRevB.95.104302

Dynamic Jahn-Teller view point for generation mechanism of low-symmetry modes of coherent phonons

Yosuke Kayanuma[1, 2, *] and Kazutaka G. Nakamura[1, †]

[1] *Laboratory for Materials and Structures, Tokyo Institute of Technology, 4259 Nagatsuta, Yokohama 226-8503, Japan*
[2] *Graduate School of Sciences, Osaka Prefecture University, 1-1 Gakuen-cho, Sakai, Osaka, 599-8531 Japan*

(Dated: February 16, 2017)

We propose a dynamic Jahn-Teller approach to elucidate the generation mechanism of low-symmetry modes of coherent phonons induced in crystals by irradiation with a short optical pulse in the opaque energy region. This is a natural extension of the impulsive excitation model of symmetric modes to multi dimensions in the configuration coordinate space. We show that the two generation mechanisms of coherent phonons coexist in this case; namely the impulsive absorption (IA) mechanism and impulsive stimulated Raman scattering (ISRS) mechanism. The dependence of the phonon amplitude on the polarization of the pump-pulse is exactly the same in IA and ISRS processes, and is in agreement with the prediction of the argument based on Raman tensors. The dependence of the excitation efficiency of the coherent phonons on the frequency of the pump-pulse is calculated using a simplified model of the optical response function of the crystal. Generally, the IA mechanism predominates in the opaque region, although ISRS makes a comparable contribution to phonon generation in the near edge opaque region. The initial phase of the coherent phonon is always cosine-like in IA, but depends on the excitation frequency in ISRS.

PACS numbers: 78.47.+p, 78.20.Bh, 63.20.Kr

I. INTRODUCTION

Irradiation of crystal surfaces with ultrashort optical pulses often induces coherent oscillation of optical phonons. These coherent optical phonons can be most conveniently observed by time-resolved pump-probe measurement of optical reflection and transmission[1–3], or x-ray diffraction[4–6]. The microscopic mechanism of generation of coherent phonons has long been a subject of central interest in this research area [7–11].

There are two well-known models for coherent phonon generation. In the impulsive stimulated Raman scattering (ISRS) mechanism, the Raman transition caused by an ultrashort optical pulse induces a transition to the excited Fock state of phonons in the electronic ground state, which is coherently overlapped with the zero-phonon state and initiates the lattice oscillation in the electronic ground state. In the displacive excitation of coherent phonon (DECP) mechanism, the coherent linear combination of the Fock state of phonons occurs in the electronic excited state. In both the ISRS and DECP models, it is tacitly assumed that there are electron-phonon interactions in the excited state, and it is necessary to excite the crystal impulsively by a pump-pulse with spectrum wider than the phonon frequency. It is generally accepted that the ISRS model is the only possible mechanism in the case of excitation in the transparent region[12].

Excitation in the opaque region is more problematic to explain, because the resonant ISRS and DECP paths should coexist according to quantum mechanics. Recently, we conducted a theoretical study using a simple two-level model to clarify the relationship between the ISRS and DECP mechanisms by applying a density matrix formalism[13]. We showed that the ISRS and DECP paths coexist as distinct quantum processes, especially in the case of resonant excitation. The amplitude of the oscillation of the optical phonon in the ISRS path is much smaller than that of DECP path when the pulse width is less than half of the period of the phonon oscillation. However, we considered only the totally symmetric phonon mode in this work.

For low-symmetry modes of optical phonons such as the E_g-mode of bismuth[14, 15], antimony[9, 16] and their compounds [17–19], it is often asserted that the generation mechanism is ISRS even in the case of pumping in the opaque region, while that of the A_{1g}-mode is assigned to DECP [14]. One of the reasons for this assignment is the experimental observation that the oscillation amplitude of the low-symmetry mode of coherent phonon depends on the polarization angle of the pump-pulse relative to the lattice coordinate, and this angular dependence agrees with that expected from the Raman tensor.

For example, take the case of the E_g-mode of Bi. For a pump-pulse incident along the z-axis , which is chosen to be parallel to the c-axis of the crystal, the Raman tensors for the E_g-mode scattering are given by

$$M_1 = \begin{pmatrix} d & 0 & 0 \\ 0 & -d & 0 \\ 0 & 0 & 0 \end{pmatrix} \quad M_2 = \begin{pmatrix} 0 & -d & 0 \\ -d & 0 & 0 \\ 0 & 0 & 0 \end{pmatrix}, \qquad (1)$$

with the definition of the linear polarized electric fields, $\vec{E}_1 \parallel \vec{e}_x$ and $\vec{E}_2 \parallel \vec{e}_y$, where $\vec{e}_x$ and $\vec{e}_y$ are the unit vectors along the x- and y- axes, respectively. The degenerated phonon modes Q_1 and Q_2 have the symmetry $Q_1 \propto x^2 - y^2$ and $Q_2 \propto -2xy$. The transition probability P_i caused

* kayanuma.y.aa@m.titech.ac.jp
† nakamura@msl.titech.ac.jp

by the Raman process described by M_i is then given by

$$P_i \propto |\vec{E}^t_{out} M_i \vec{E}_{in}|^2, \tag{2}$$

where $\vec{E}_{in}$ and $\vec{E}_{out}$ are the electric fields of the incident and scattered light, respectively, and $\vec{E}^t_{out}$ means the transpose of $\vec{E}_{out}$. In the pump-process involving ISRS, we set $\vec{E}_{in} = \vec{E}_{out} = \vec{E} \propto \cos\theta \vec{e}_x + \sin\theta \vec{e}_y$ where θ is the angle between the polarization of the pump-field $\vec{E}$ and the x-axis. Then we find the polarization dependence of the scattering amplitude S_1 and S_2 by the generation of the E_g phonons Q_1 and Q_2 given by

$$\begin{aligned} S_1 &\propto d\cos 2\theta, \\ S_2 &\propto -d\sin 2\theta. \end{aligned} \tag{3}$$

In the case of coherent phonons, the generated E_g-mode phonons modulate the electric susceptibility, which can be probed as a pump induced change of the transient reflectivity or transmissivity. The signal amplitudes caused by the low-symmetry modes are generally much smaller than that induced by the symmetric mode. We may select the signals assigned to each phonon mode by electro-optic measurement with a suitable choice of the crystal axis. The agreement of the observed angular dependence of the pump-pulse in the signal of the coherent phonons with the prediction by the Raman tensors[14, 18] seems to suggest that the generation mechanism is ISRS. However, it should be stressed that this agreement does not necessarily confirm that the microscopic origins of the two distinct processes of the resonant Raman scattering by a stationary field and coherent phonon generation by a pump-pulse are the same.

For the theoretical studies of generation mechanism of coherent phonons, Zeiger and coworkers[7] proposed in their pioneering work a phenomenological model based on a semiclassical equation of motion. Kuznetsov and Stanton[8] studied the microscopic origin of coherent motion of phonons on the electron-phonon coupled Hamiltonian. They derived an equation of motion for the coherent amplitude of the annihilation operator of phonons by the Heisenberg equation of motion. Since the Heisenberg equation for harmonic oscillators has essentially the same structure as the classical counterpart, their results allow an intuitive understanding of the generation mechanism. Here, only the DECP process for fully symmetric mode was included.

In the work by Garrett and coworkers[9], Merlin[10] and Stevens *et al.*[11], theory was extended to cover also the case of multiple bands in the excited state. In these works too, the semiclassical equation of motion of the phonon coordinates plays a central role. The distinction between DECP and ISRS was included in the difference of the force term. In ref.[11], it was asserted that the notion of DECP is not a distinct mechanism, but a particular case of stimulated Raman scattering. However, this statement is confusing because the final states of the electronic system is different between DECP and ISRS. The optical absorption is not a particular case of the Raman scattering.

In the present work, we propose a different approach to the problem of coherent phonon generation with special attention to the case of low-symmetry mode. Before going into details, we adopt henceforth a term impulsive absorption (IA) instead of DECP, because the term DECP has been used only in the case of fully symmetric mode[8]. The difference between IA and ISRS is whether the excited electron occupies the excited state (IA) or has returned to the ground state (ISRS) after the passage of the pump-pulse. Therefore, DECP is a particular case of IA.

In this work, we use a simplified band model to elucidate the generation process of the coherent phonons of low-symmetry modes with the dynamic Jahn-Teller interaction. We don't resort to the equation of motion of the phonon coordinate, but directly calculate the density matrix for the electron-phonon coupled system and the expectation value of the phonon amplitude on the assumption that the coupling constant is weak. We then discuss the dependence of the phonon amplitude on the polarization of the pump-pulse. We find that, as observed previously[13], the IA and the ISRS paths coexist as distinct quantum processes, and both display the same dependence of the amplitude of the coherent phonons on the polarization angle. The IA mechanism predominates over the ISRS process with respect to the generation efficiency in the opaque region except for the case of excitation to the band-edge, where the IA and ISRS processes compete in terms of the generation efficiency. Furthermore, we revealed that the initial phase of the oscillation of coherent phonon is always cosine-like in the IA path, while it depends on the frequency of the pump-pulse in the ISRS process.

II. MODEL

First, it should be noted that behind the Raman tensors, a set of electron-phonon interactions with the same symmetry exists, from which the Raman tensors are derived[20]. In the case of low-symmetry modes, this interaction works between the degenerate electronic states that transform as a distinct basis set in an irreducible representation of the crystal. In 1937, Jahn and Teller[21] proved a theorem that if a symmetric non-linear molecule has a degenerate electronic states, it distorts in such a way to remove the electronic degeneracy. This effect is called a static Jahn-Teller effect, because the atomic degrees of freedom were treated as classical variables which define the static adiabatic potentials. The dynamic aspect of the Jahn-Teller effect was then studied in which the quantum mechanical interaction between the electronic and atomic degrees of freedom was a subject of interest[22]. The concept of Jahn-Teller interaction was extended to localized centers in solids[23]. For example, the splitting of the optical absorption band in some heavy

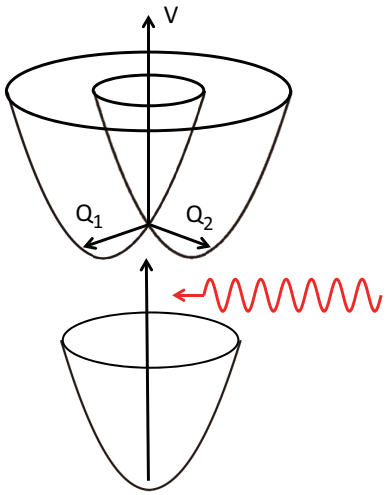

FIG. 1. Adiabatic potential energy surface for the Jahn-Teller interaction with E_g-mode phonons (top). Potential surface of the ground state (bottom).

metal ions doped in alkali halides is explained theoretically as a result of the Jahn-Teller interaction between the localized electronic states with the low-symmetry distortion of the surrounding ions[24].

Another extension of the Jahn-Teller scenario is the band Jahn-Teller effect, which is closely related to our work. In the band Jahn-Teller model, a set of symmetry-degenerated band of itinerant electrons are coupled locally with low-symmetry phonon modes. This is motivated to explain the origin of $d-d$ interaction in cuprate superconductors[25–27]. In the present work, we apply the dynamic Jahn-Teller interaction model of band electrons to the coherent phonon generation of low-symmetry phonons. Although the following argument can be easily extended to general types of Jahn-Teller interactions, we consider here the case of E_g-mode coupled with a set of electronic states with two-dimensional representation for concreteness.

First we derive our model Hamiltonian in a simplified form. We consider an optical pumping of a uniaxial semiconductor or semimetal. For simplicity, the sample is assumed to be a slab of single crystal with size $L \times L \times L'$, where L is the length of sides and L' is the thickness. It is assumed that the crystal surface is perpendicular to the c-axis, and the pump-pulse hits the surface along the normal direction of the surface. For the model of the electronic state, it is assumed that the valence band is composed of even parity s-like states, and the conduction band is degenerate with x-like states and y-like states with odd-parity. The Hamiltonian is given by

$$H_e = \sum_{\vec{k}} \epsilon_v(k) a^\dagger_{k,s} a_{k,s} + \sum_{\vec{k}} \sum_{\xi=x,y} \epsilon_c(k) a^\dagger_{k,\xi} a_{k,\xi}, \quad (4)$$

where $a_{k,s}$ and $a_{k,\xi}(\xi = x, y)$ are the annihilation operator for the Bloch electrons of the valence band with s-like symmetry and energy $\epsilon_v(k)$, and the conduction band with ξ-like symmetry and the energy $\epsilon_c(k)$, respectively. The two-fold degenerate conduction band is called an e-band.

The electronic states in the conduction band are assumed to be locally coupled with E_g-mode phonons as described by the Hamiltonian

$$H_{eL} = c \sum_j \Big\{ Q^j_1 \left(a^\dagger_{j,x} a_{j,x} - a^\dagger_{j,y} a_{j,y} \right) - Q^j_2 \left(a^\dagger_{j,x} a_{j,y} + a^\dagger_{j,y} a_{j,x} \right) \Big\}, \quad (5)$$

where Q^j_λ $(\lambda = 1, 2)$ is the coordinate of the λ-component of E_g-phonon at j-th unit cell, c is the coupling constant, and $a_{j,\xi}$ is the annihilation operator for the Wannier state at j-th unit cell which is given by

$$a_{j,\xi} = \frac{1}{\sqrt{N}} \sum_{\vec{k}} a_{k,\xi} e^{-i\vec{k}\cdot\vec{R}_j}, \quad (6)$$

in which N is the number of unit cells in the crystal, $\vec{R}_j$ is the lattice vector for the j-th unit cell, and the summation $\sum_k$ should be taken over the points in the first Brillouin zone. Likewise the phonon coordinate is expanded into the normal modes as

$$Q^j_\lambda = \sum_{\vec{q}} \sqrt{\frac{\hbar}{2NM\omega_q}} \Big\{ b_{\lambda,q} e^{i\vec{q}\cdot\vec{R}_j} + b^\dagger_{\lambda,q} e^{-i\vec{q}\cdot\vec{R}_j} \Big\}, \quad (7)$$

in which M is the reduced mass of atoms per a unit cell, ω_q is the frequency of the optical phonons, and $\left(b_{\lambda,q}, b^\dagger_{\lambda,q} \right)$ are the annihilation and the creation operators for the normal mode satisfying the commutation relation

$$[b_{\lambda,q}, b^\dagger_{\lambda',q'}] = \delta_{q,q'} \delta_{\lambda,\lambda'}. \quad (8)$$

Inserting Eqs. (6), (7) into (5), we rewrite (5) as

$$H_{eL} = c\sum_{\vec{q}}\sum_{\vec{k}}\frac{1}{\sqrt{2NM\omega_q}}\Big\{\left(b^\dagger_{1,q}+b_{1,-q}\right)\left(a^\dagger_{k+q,x}a_{k,x}-a^\dagger_{k+q,y}a_{k,y}\right) - \left(b^\dagger_{2,q}+b_{2,-q}\right)\left(a^\dagger_{k+q,x}a_{k,y}+a^\dagger_{k+q,y}a_{k,x}\right)\Big\}. \quad (9)$$

The Hamiltonian for the phonon energy is written as

$$H_L = \sum_{\vec{q}}\hbar\omega_{\vec{q}}\left(b^\dagger_{1,q}b_{1,q}+b^\dagger_{2,q}b_{2,q}\right), \quad (10)$$

where $\hbar\omega_{\vec{q}}$ is the energy of the E_g-mode phonon.

It should be noted here that, according to the phase matching, the wave vectors of phonons which can be excited by the optical processes are only those lying close to the Γ-point $\vec{q}=0$ because the optical wave-length is much larger than the lattice constant. The eigen modes of phonons form a continuum around $\vec{q}=0$. The electromagnetic field interacts only with the atoms within the penetration depth $\delta L'$. In the opaque region, $\delta L'$ is usually much smaller than the crystal thickness L'. This effect relaxes the condition of phase matching and allows the modes with $\delta q \sim 1/\delta L'$ around $\vec{q}=0$ to be excited[9]. Furthermore, the pump-pulse is focused on the spot size which is smaller than the surface area size L. This means that the phase matching condition along the lateral direction is also relaxed.

We may roughly classify all of the normal modes into two; the $2N'$ active modes around $\vec{q}=0$ which are excited by the optical pulses, and $2(N-N')$ inactive modes which are not excited. Then the model Hamiltonian is greatly simplified by taking into account only the active modes as follows. We define the creation operators for the *interaction modes* $b^\dagger_\lambda \quad (\lambda=1,2)$ by

$$b^\dagger_\lambda \equiv \beta{\sum_{\vec{q}}}' b^\dagger_{\lambda,q}, \quad (\lambda=1,2), \quad (11)$$

where the summation $\sum'_{\vec{q}}$ runs over the N' active modes around $\vec{q}=0$. The constant β is determined by the normalization condition,

$$[b_\lambda, b^\dagger_\lambda] = \beta^2 N' = 1, \quad (12)$$

as $\beta = 1/\sqrt{\rho N}$, where $\rho \equiv N'/N << 1$ is the fraction of the phase space volume occupied by the active modes. Dropping the inactive modes from the summation (9), and approximating $\vec{q}=0$ for the active modes, we find

$$H_{eL} = \alpha\hbar\omega\sum_{\vec{k}}\Big\{\left(b^\dagger_1+b_1\right)\left(a^\dagger_{k,x}a_{k,x}-a^\dagger_{k,y}a_{k,y}\right) - \left(b^\dagger_2+b_2\right)\left(a^\dagger_{k,x}a_{k,y}+a^\dagger_{k,y}a_{k,x}\right)\Big\}, \quad (13)$$

where we set $\omega_{\vec{q}=0}=\omega$, and α is the dimensionless coupling constant

$$\alpha = c\frac{1}{\hbar\omega}\sqrt{\frac{\rho\hbar}{2M\omega}}. \quad (14)$$

Note that α is independent of the system size N. Note also that it depends not only on the material constants but also on the experimental condition.

We have selected only two modes out of the $2N'$-dimensional subspace of active modes. The concept of the interaction mode was introduced into the theory of Jahn-Teller effects in localized centers by Toyozawa and Inoue[24] and O'Brien[28] in a slightly different context. Other $2N'-2$ modes can be defined within this subspace by an orthogonal transformation of the phonon variables to be orthogonal each other and also with the interaction mode. Because the original modes $\left(b^\dagger_{\lambda,q}, b_{\lambda,q}\right)$ are normal modes, this transformation may give rise to the bilinear off-diagonal coupling between the new variables through the dispersion of energy in the Hamiltonian (10). It can be proven that it is always possible to choose this orthogonal transformation so as the off-diagonal couplings to appear only between the interaction modes and the rest modes. The $2N'-2$ rest modes are then regarded as forming a reservoir modes for the interaction modes, and induces the relaxation of the coherent motion of the interaction modes[29]. In the present case, however, the off-diagonal coupling is considered small, because the original modes are optical modes in the vicinity of Γ-point. In the present work, we neglect this coupling, and simply rewrite H_L by taking into account only the interaction modes,

$$H_L = \hbar\omega\left(b^\dagger_1 b_1 + b^\dagger_2 b_2\right). \quad (15)$$

Mode 1 and 2 correspond to the two Raman-mode phonons described in Eq.(1). It is easily ascertained by a first order perturbation calculation with respect to H_{eL} that the above Hamiltonian reproduces the Raman selection rule Eq. (1) in the continuous-wave Raman scattering.

If we define the configuration coordinates and their conjugate momenta for the E_g interaction modes by

$$Q_\lambda = \sqrt{\frac{\hbar}{2M\omega}}\left(b^\dagger_\lambda + b_\lambda\right), \quad P_\lambda = i\sqrt{\frac{M\hbar\omega}{2}}\left(b^\dagger_\lambda - b_\lambda\right), \quad \lambda=1,2, \quad (16)$$

the adiabatic potential $V(Q_1,Q_2)$ for the excited state with a fixed value of k is given as

$$V(Q_1,Q_2) = \frac{M\omega^2}{2}\left(Q_1^2+Q_2^2\right) \pm \alpha\omega\sqrt{2M\hbar\omega}\sqrt{Q_1^2+Q_2^2}. \quad (17)$$

In Fig. 1, $V(Q_1, Q_2)$ is illustrated schematically[22, 23] together with the adiabatic potential of the ground state. $V(Q_1, Q_2)$ has a conical intersection at $Q_1 = Q_2 = 0$. The relaxation energy is $\alpha^2\hbar\omega$. The eigenvalue problem for the vibronic system under the Hamiltonian $H_e + H_L + H_{eL}$ and its optical responses are called an $E\otimes e$-problem and have been studied extensively for some decades[22, 24].

For the interaction Hamiltonian with the pump-pulse, we take

$$H_{eR}(t) = Ef(t)\sum_k \mu_k(\cos\theta a^\dagger_{k,x}a_{k,s} + \sin\theta a^\dagger_{k,y}a_{k,s})e^{-i\Omega_0 t} + H.c., \quad (18)$$

where $f(t)$ is the dimensionless pulse-envelope localized around $t = 0$, $\Omega_0 (>> \omega)$ is the central frequency of the pump-pulse with field strength E, and μ_k is the transition dipole moment. Here we approximated that the optical transition takes place vertically in the Brillouin region. In actual calculations, we used the Gaussian pulse with the pulse-width σ,

$$f(t) = \frac{1}{\sqrt{\pi}\sigma\Omega_0}\exp\left(-t^2/\sigma^2\right). \quad (19)$$

We consider the resonant impulsive excitation and deexcitation processes by $H_{eR}(t)$ under the condition that $\hbar\Omega_0$ exceeds the band-gap energy. In this work, we are interested in the possible mechanisms of coherent phonon generation and, especially, in the initial amplitude of phonon oscillation. Therefore, we simply neglect various relaxation pathways for the electrons and phonons.

III. RESULTS AND DISCUSSION

It is assumed that the system was initially in the ground state with zero phonon, described by the ket vector $|\psi(-\infty)\rangle = |g\rangle \otimes |0\rangle$ where $|g\rangle$ is given by $|g\rangle = \prod_k a^\dagger_{k,s}|\text{vac}\rangle$ with $|\text{vac}\rangle$ being the vacuum of electron, and $|0\rangle$ is the vacuum of phonon.

If we set the unperturbed Hamiltonian H_0 as

$$H_0 = H_e + H_L, \quad (20)$$

the temporal development of the ket vector under the electron-photon and electron-phonon interactions obeys the Schrödinger equation

$$i\hbar\frac{d}{dt}|\psi(t)\rangle = (H_0 + H_{eR}(t) + H_{eL})\,|\psi(t)\rangle, \quad (21)$$

which is formally solved as

$$|\psi(t)\rangle = \exp\left(-\frac{i}{\hbar}H_0 t\right)\exp_+\left(-\frac{i}{\hbar}\int_{-\infty}^{t}\left\{\tilde{H}_{eR}(t') + \tilde{H}_{eL}(t')\right\}dt'\right)|\psi(-\infty)\rangle, \quad (22)$$

where $\exp_+$ means the time-ordered exponential and $\tilde{H}_{eR}(t)$ and $\tilde{H}_{eL}(t)$ are given by

$$\tilde{H}_{eR}(t) = e^{iH_0 t/\hbar}H_{eR}(t)e^{-iH_0 t/\hbar},$$
$$\tilde{H}_{eL}(t) = e^{iH_0 t/\hbar}H_{eL}e^{-iH_0 t/\hbar}, \quad (23)$$

respectively.

We calculate the density matrix $\rho(t) = |\psi(t)\rangle\langle\psi(t)|$ to the lowest order perturbation expansion with respect to $\tilde{H}_{eR}(t)$ and $\tilde{H}_{eL}(t)$ that gives nonzero expectation values of $Q_1(t)$ and $Q_2(t)$. The double-sided Feynman diagrams for the density matrices corresponding to the IA and ISRS processes are shown in Fig. 2. In these diagrams, the temporal evolution of the ket (bra) vectors is shown in the upper (lower) propagators. The time runs from $-\infty$ (far left) to t (far right). The filled circles indicate the vertices of the absorption and emission of photons. The empty circles are the vertices of emission of phonon 1 or 2, which are indicated by dashed lines. Figure 2 (a) - (d) correspond to the processes that contribute to $\langle Q^{(A)}_\lambda(t)\rangle$ and $\langle Q^{(S)}_\lambda(t)\rangle$ $(\lambda = 1, 2)$, where (A) and (S) represent the IA and ISRS paths, respectively. The Hermitian conjugate diagram, which is obtained by interchanging the upper and the lower propagators, is also indicated for each diagram.

The time-ordered integral should be carried out for both photon and phonon vertices. The subspace of the excited states is composed of $|\vec{k}, \xi\rangle \otimes |0\rangle$ and $|\vec{k}, \xi\rangle \otimes |1_\lambda\rangle$ where $|\vec{k}, \xi\rangle = a^\dagger_{k,\xi}a_{k,s}|g\rangle$ and $|1_\lambda\rangle = b^\dagger_\lambda|0\rangle$, $(\xi = x, y, \quad \lambda = 1, 2)$. Inspection of the interaction Hamiltonians $\tilde{H}_{eR}(t)$ and $\tilde{H}_{eL}(t)$ reveals the following rule for assignment of factors: Assign $\cos\theta$ $(\sin\theta)$ to each photon-vertex connecting $|g\rangle$ with $|\vec{k}, x\rangle$ ($|g\rangle$ with $|\vec{k}, y\rangle$). Assign α to each phonon-vertex connecting $|\vec{k}, x\rangle$ with $|\vec{k}, x\rangle$. Assign $-\alpha$ to each phonon-vetex connecting $|\vec{k}, y\rangle$ with $|\vec{k}, y\rangle$ and $|\vec{k}, x\rangle$ with $|\vec{k}, y\rangle$.

The calculation was performed for time t well after the passage of the pump-pulse $t >> \sigma$, allowing us to determine the expectation values for the phonon coordinates,

$$\langle Q^{(A)}_1(t)\rangle = A(t)\cos 2\theta,$$
$$\langle Q^{(A)}_2(t)\rangle = -A(t)\sin 2\theta,$$
$$\langle Q^{(S)}_1(t)\rangle = S(t)\cos 2\theta,$$
$$\langle Q^{(S)}_2(t)\rangle = -S(t)\sin 2\theta, \quad (24)$$

in which

$$A(t) = L_A(\Omega_0)\left(e^{-i\omega t} + e^{i\omega t}\right) - 2\Delta, \tag{25}$$

$$S(t) = L_S(\Omega_0)e^{-i\omega t} + L_S^* e^{i\omega t}, \tag{26}$$

with

$$L_A(\Omega_0) = D\int_{-\infty}^{\infty} du e^{-\frac{u^2}{2\sigma^2}} e^{i(\Omega_0 - \frac{\omega}{2})u} F(u), \tag{27}$$

$$L_S(\Omega_0) = 2iD\int_0^{\infty} du e^{-\frac{u^2}{2\sigma^2}} \sin(\omega u/2)\, e^{i\Omega_0 u} F(u) \tag{28}$$

In the above equations, $\langle\cdots\rangle$ means that the expectation value over the electronic and phononic states should be taken,

$$D = \alpha\sqrt{\frac{\hbar}{2M\omega}}\left(\frac{E}{\hbar\Omega_0}\right)^2 \frac{1}{\sqrt{2\pi}\sigma} e^{-\sigma^2\omega^2/8},$$

$$\Delta = \alpha\sqrt{\frac{\hbar}{2M\omega}}\left(\frac{E}{\hbar\Omega_0}\right)^2 \frac{1}{\sqrt{2\pi}\sigma}\int_{-\infty}^{\infty} du e^{-\frac{u^2}{2\sigma^2} - i\Omega_0} F(u),$$

and $F(u)$ is the response function defined by

$$F(u) = \sum_k |\mu_k|^2 e^{-i\epsilon_k u/\hbar - \gamma|u|}, \quad (\gamma = 0^+) \tag{29}$$

in which $\epsilon_k \equiv \epsilon_c(k) - \epsilon_v(k)$. The term Δ corresponds to the shift of the equilibrium of phonons in the excited state. The derivation of the above formulas is given in the Appendix.

It should be noted that $F(u)$ can be obtained once the absorption spectrum $I(\Omega) = \sum_k |\mu_k|^2\delta(\Omega - \epsilon_k/\hbar)$ corresponding to the e-band is known: $F(\Omega)$ is given by its Fourier transform,

$$F(u) = \int_{-\infty}^{\infty} I(\Omega)e^{-i\Omega u} d\Omega. \tag{30}$$

The Laplace transform of $F(u)$

$$\chi(\Omega) \equiv i\int_0^{\infty} F(u)e^{i\Omega u} du \tag{31}$$

is the optical susceptibility which describes the response to stationary fields. We define the pulse suceptibility $\chi_p(\Omega)$ by

$$\chi_p(\Omega) \equiv i\int_0^{\infty} e^{-\frac{u^2}{2\sigma^2}} F(u)e^{i\Omega u} du. \tag{32}$$

Then Eqs.(27) and (28) can be written as

$$L_A(\Omega_0) = \frac{1}{i}D\left\{\chi_p(\Omega_0 - \frac{\omega}{2}) - \chi_p^*(\Omega_0 - \frac{\omega}{2})\right\}, \tag{33}$$

$$L_S(\Omega_0) = D\left\{\chi_p(\Omega_0 + \frac{\omega}{2}) - \chi_p(\Omega_0 - \frac{\omega}{2})\right\}. \tag{34}$$

As shown here, the expectation values of the phonon coordinates are factorized into products of the dynamical factors, $A(t)$ and $S(t)$ and the geometrical factors $\cos 2\theta$ and $\sin 2\theta$. The dynamical factors found here are essentially the same as those for the case of interaction with a totally symmetric mode. To recover the formulas for the symmetric mode, we need only set $\theta = 0$ formally in Eq. (24), change the value of coupling constant α appropriately, and reinterpret Q_1 as the coordinate for the symmetric mode. Then, in the limit of zero band-width, $\langle Q_1^{(A)}(t)\rangle$ and $\langle Q_1^{(S)}(t)\rangle$ reduce to those obtained in Eqs. (19) and (22), respectively, in our previous work [13].

An important point is the fact that the geometrical factors for the IA and ISRS processes are the same. This is easily ascertained from the diagrams shown in Fig. 2. Although the final electronic states of the IA and ISRS processes are different, there is a correspondence between

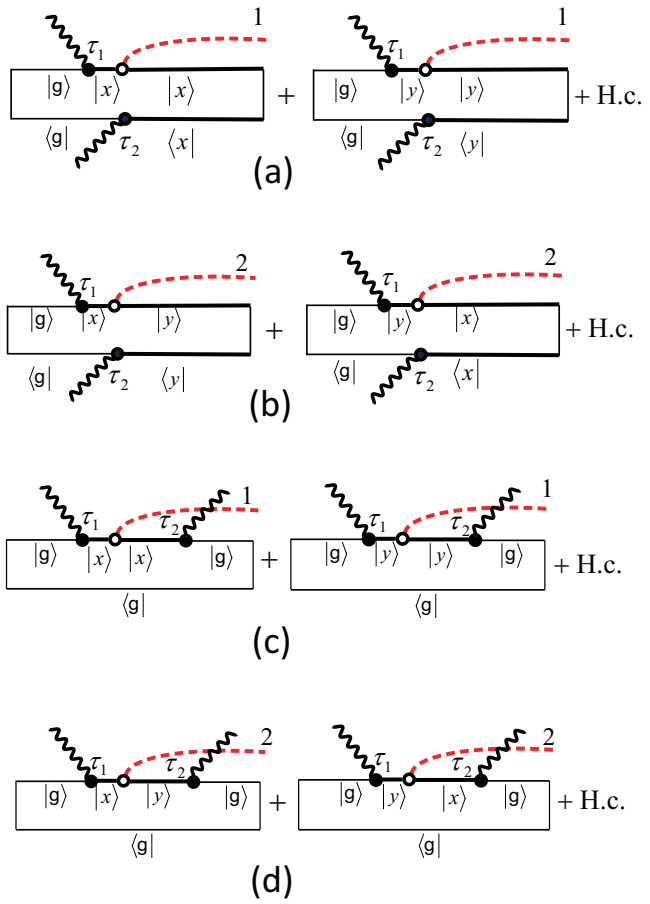

FIG. 2. Double-sided Feynman diagrams representing the photo-induced processes, (a) and (b) IA, and (c) and (d) ISRS. The upper and lower lines represent the time-evolution of the ket and bra vectors, respectively. Thin lines represent the electronic ground state and thick lines the excited states $|x\rangle$ and $|y\rangle$. Wavy lines represent photons and dashed lines represent E_g-mode phonons 1 and 2. The filled circles indicate the vertices of the absorption and emission of photons. The empty circles are the vertices of emission of phonon 1 or 2, which are indicated by dashed lines. Time runs from left to right.

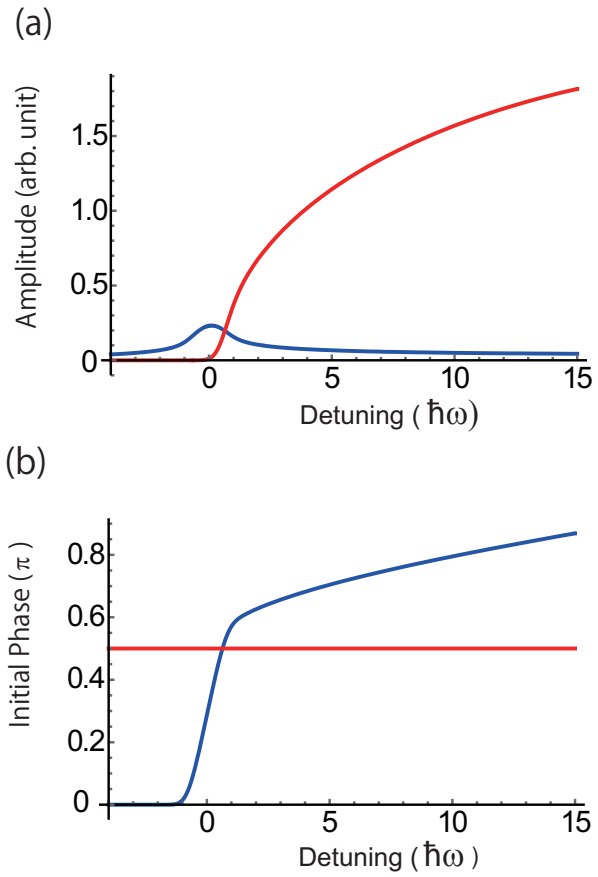

FIG. 3. (Color online) (a) Amplitude of coherent phonons as a function of the central frequency of the pump-pulse measured from the absorption edge. The band-width is assumed to be $50\hbar\omega$, and the pulse-width is $\sigma = \pi/\omega$. Both IA (red line) and ISRS (blue line) processes are plotted. (b) Initial phase of coherent phonons for the IA (red) and ISRS (blue) processes. The values of B and σ are the same as those in (a).

Fig. 2 (a) and (c), and (b) and (d); for example, the left diagram in (a) is topologically equivalent to the left diagram in (c) if one traces the evolution of the state clockwise from $-\infty$ to t, then from t to $-\infty$. Thus, the polarization dependence of the coherent phonon amplitude is identical in both IA and ISRS processes as shown in Eq. (24).

Stevens and coworkers[11] have shown a formula for the generation amplitude of A_{1g} coherent phonons in Sb based on their theoretical frame work[9, 10]. In their theory, the equation of motion for the phonon coordinates is derived in the Heisenberg picture. The force term to this equation contains the operators for the electrons. This term was evaluated by the zeroth order approximation. Therefore, the theory is essentially a perturbation theory to the lowest order of the electron-phonon interaction. This is the same as the present theory based on the Schrödinger picture. Our formulas (33) and (34) seem to be similar to the two-Raman tensor formula in [11], if one takes the sum $\langle Q(t)\rangle = \langle Q_1^{(A)}(t)\rangle + \langle Q_1^{(S)}(t)\rangle$, except for a discrepancy in the arguments by the amount of $\omega/2$[30]. However, it will be advantageous to consider the two quantum mechanically different processes, IA and ISRS, distinctly as was done here. This is especially true when we analyze the experimental data in which not only the coherence of phonons but also the coherence of the electronic states are being measured and controlled by a double-pulse technique[31], because the IA and ISRS pathways give rise to quite different temporal profiles of interference. Details will be presented elsewhere[32].

Let us discuss the excitation energy dependence of the generation efficiency of coherent phonons and their initial phase. To reveal the essential features, we assume that the absorption spectrum of the e-band is a simple hemielliptic band,

$$\begin{aligned} I(\Omega) &= I_0\sqrt{(\Omega-\Omega_l)\,(\Omega_u-\Omega)},\ \Omega_l \le \Omega \le \Omega_u, \\ &= 0,\ \text{otherwise}, \end{aligned} \tag{35}$$

where $\hbar\Omega_l$ and $\hbar\Omega_u$ are the lower and upper band-edges, respectively, and I_0 is a constant. From Eq.(30), we find

$$F(u) = I_0 e^{-i(\hbar\Omega_l+B)u/\hbar}\frac{B}{\hbar u}J_1(Bu/\hbar), \tag{36}$$

where B is the half-band width, $B = \hbar(\Omega_u - \Omega_l)/2$, and $J_1(x)$ is the first order Bessel function.

In Fig. 3 (a), the calculated generation efficiencies of coherent phonons for the IA (red line) and ISRS (blue line) processes are shown as a function of the detuning $\hbar(\Omega_0 - \Omega_l)$ normalized by the phonon energy $\hbar\omega$. The chosen band-width $2B$ was $2B = 50\hbar\omega$. The pulse width was assumed to be $\sigma = \pi/\omega$. Figure 3 (a) reveals that the amplitude of the coherent phonon caused by the IA process is almost proportional to the absorption spectrum $I(\Omega)$. To be more precise, it is proportional to the convolution of $I(\Omega)$ with the Gaussian function $\tilde{f}(\omega') = \exp\left[-\sigma^2\omega'^2/2\right]$ as

$$|L_A(\Omega_0)| \propto \int_{-\infty}^{\infty} I(\Omega_0 - \frac{\omega}{2} - \omega')\tilde{f}(\omega')d\omega'. \tag{37}$$

As can be seen in Fig. 3 (a), the amplitude due to IA rises up not at the band edge Ω_l but at $\Omega_l + \omega/2$. The physical reason is that, to induce a coherent motion of phonons in the excited state, it is necessary to excite both the zero-phonon state and the one-phonon state simultaneously.

In contrast, the ISRS component $|L_S|$ becomes appreciable only at the absorption edge, or more generally, around the van Hove singularities. This is because $L_S(\Omega_0)$ is proportional to the difference of $\chi_p(\Omega_0)$ at $\Omega_0 \pm \omega/2$ as shown in Eq. (34). Therefore, $L_S(\Omega_0)$ becomes small in the region where $I(\Omega)$ is smoothly varying. Deep into the opaque region, IA predominates, while in the transparent region, only ISRS contributes to the generation of coherent phonons. It is noticeable that both the IA and ISRS paths coexist with comparable magnitudes of generation efficiency in the band-edge region.

The initial phase of coherent phonon is sometimes considered to be a clue to the generation mechanism. The initial phase ϕ is determined experimentally[9, 14, 18, 34] by fitting the oscillation of the transient reflectivity $\Delta R(t)$ (or transmissivity) by the sinusoidal function as

$$\Delta R(t) = \Delta R^0 \sin(\omega t + \phi), \tag{38}$$

in which t is the delay-time of the probe pulse measured from the pump pulse and ΔR^0 is the amplitude of oscillation. It is often asserted that, in the case of IA, the oscillation is cosine-like; namely $\phi = \pi/2$ with modulus π. Conversely, in the case of ISRS, the oscillation is sine-like, $\phi = 0$ with modulus π. This seems to be in agreement with the simple picture of the generation of coherent phonons; The IA process occurs because of the sudden shift of the equilibrium configuration for the phonons, while the ISRS process is triggered by the sudden acquirement of momentum induced by the stimulated Raman scattering. However, it should be noted that, in the case of resonant excitation in the opaque region, it takes a finite time for the Raman process to occur effectively in ISRS[13].

From Eq. (33), it is obvious that L_A is a real quantity. Thus, according to Eq.(25), the oscillation by the IA process is always cosine-like; namely $\phi = \pi/2$. In contrast, $L_S(\Omega_0)$ is a complex quantity. The initial phase ϕ was obtained by putting $L_S(\Omega_0)$ in the form

$$L_S(\Omega_0) = |L_S(\Omega_0)| \exp\left[i(\phi + \frac{\pi}{2})\right]. \tag{39}$$

In Fig. 3 (b), the calculated values for the initial phase are plotted as functions of the central frequency Ω_0 of the pump-pulse. The initial phase of coherent phonons formed by the IA process is always $\pi/2$, as noted above. However, the initial phase for ISRS depends on the frequency of the pump-pulse. In the transparent region, $\phi = 0$ and the oscillation is sine-like. As Ω_0 traverses the absorption edge, the initial phase changes rapidly, and then increases gradually in the opaque region until it reaches 2π after Ω_0 traverses the whole absorption band.

We found that the polarization-angle dependence of the coherent-phonon amplitude cannot be used as a key to differentiate the generation mechanism of the low-symmetry mode, because it is always in agreement with the prediction by the Raman tensor. Considering the relative magnitude of the oscillation, the IA mechanism is a dominant pathway in the case of excitation far into the opaque region. Furthemore, IA also predominates in the limit of short pulse excitation[13].

As for the initial phase of the oscillation, we demonstrated that IA and ISRS behave distinctly. The initial phase in the IA path is always cosine-like, but that in the ISRS depends on the excitation energy. It is suspected that this is one of the reasons why the experimental measurements of the initial phase give diverse results[9]. In the transparent region, ISRS is the only mechanism that generates coherent phonons and their initial phase is sine-like. This appears to be in agreement with the observation for the uniaxial wide-gap materials such as GaN[33], ZnO[34], CdS[35] and α-quartz[36].

According to the dynamic Jahn-Teller model, the amplitude of the coherent phonon is expected to be proportional to that of the resonant Raman scattering. One of the method to ascertain this criterion is to compare the ratio of the amplitude between the A_{1g}-mode and E_g-mode in the Fourier transform of the coherent phonons and the Raman scattering measured for the excitation to the same band. In the case of Sb, a good agreement has been reported for the excitation wavelength $\lambda = 815$nm [9]. In the case of Bi_2Te_3, on the other hand, a large discrepancy between the ratio has been reported[37]. One of the possible origin is the difference in the relaxation processes during and after the irradiation of pump-pulse[38]. Detailed investigation in experiment and in theory should be needed to clarify this point.

In experimental observations of the coherent phonons in uniaxial materials, the signals corresponding to the low-symmetry modes are generally very weak compared with those for the symmetric modes. The main reason for this is attributed to the difference in the magnitude of the electron-phonon coupling constants of the modes. In the case of symmetric A_{1g}-mode, the electron-phonon coupling is roughly proportional to the difference of the charge distribution between the ground state and excited states. Conversely, the dynamic Jahn-Teller interaction works between the electronic states that are both in the excited-state subspace. This will decrease the off-diagonal coupling constant in the dynamic Jahn-Teller effect. As observed by Melnikov *et al.*[15], the generation efficiency of the E_g-mode phonons is expected to have different excitation-energy dependence from that for the A_{1g}-mode ones because of the different symmetry of the excited states. To resolve the long lasting controversy over the generation mechanism of coherent phonons, especially for low-symmetry modes, it is desirable to perform a careful experiment to determine the initial phase by sweeping the pump-pulse across the band-edge.

IV. CONCLUSION

The generation mechanism of the low-symmetry mode of coherent phonons was considered under the condition that a short pump-pulse in the opaque wave-length region excites the electronic system. Using a simplified model for the E_g-mode in bulk crystals, we showed that the two distinct mechanisms IA and ISRS coexist quantum mechanically. We found that both mechanism displayed essentially the same dependence of the oscillation amplitude of phonons on the relative polarization of the pump-pulse, in agreement with the prediction by the Raman tensor. The IA process predominates in far above-band-gap excitation, while the ISRS mechanism plays an important role in the case of excitation to the near-threshold

region.

The present theory indicates that the generation processes of coherent phonons of the totally symmetric A_{1g}-mode and low-symmetry E_g-mode can be formulated on essentially the same footing. In fact, the formulas for the dynamic factors $A(t)$ and $S(t)$ given in Eqs. (24) and the arguments on the generation efficiency and initial phase presented here are also valid for A_{1g}-mode phonons. This is a consequence of the assumption that the electron-phonon coupling is weak so that the lowest order perturbation theory is applicable, which yields formally the same expressions for the dynamical factors.

In the present work, we restricted ourselves to elucidating the generation process of coherent phonons. The detection process can be also formulated within the same model Hamiltonian. In the analyses of experimental data, however, it is necessary to take into account various relaxation processes appropriately, because the pump-probe delay time is typically as long as some picosecond. Among others, the intra-band and inter-band scattering of the electrons excited by the IA process are expected to be very fast. This will result in the difference in the fate of coherent phonons created via IA and ISRS, because in ISRS, the electronic system returns to the initial configuration just after the pump-pulse with only phonons remaining in crystal. From experiment side, it will be a challenge to work out techniques to observe coherent phonons discriminating the IA-path and ISRS-path.

ACKNOWLEDGMENTS

This work was partially supported by Core Research for Evolutional Science and Technology (CREST) of the Japan Science and Technology Agency, JSPS KAKENHI Grant Number 15H02103, 15K13377, 16K05396, and the Collaborative Research Project of Laboratory for Materials and Structures.

[1] Y.-X. Yan, E. B. Gamble, and K. Nelson, J. Chem. Phys. **83**, 5391 (1985).
[2] G. C. Cho, W. Kütt, and H. Kurz, Phys. Rev. Lett. **65**, 764 (1990).
[3] T. Dekorsy, T. Pfeifer, W. Kütt, and H. Kurz, Phys. Rev. B **47**, 3842 (1993).
[4] K. Sokolowski-Tinten, C. Blome, J. Blums, A. Cavalleri, C. Dietrich, A. Tarasevitch, I. Uschmann, E. Förster, M. Kammler, M. Horn-von-Hoegen, and D. von der Linde, Nature, **422**, 287 (2003).
[5] K. G. Nakamura, S. Ishii, S. Ishitsu, M. Shiokawa, H. Takahashi, K. Dharmalingam, J. Irisawa, Y. Hironaka, K. Ishioka, and M. Kitajima, Appl. Phys. Lett. **93**, 061905 (2008).
[6] S. L. Johnson, P. Beaud, E. Möhr-Vorobeva, A. Caviezel, G. Ingold, and C. J. Milne, Phys. Rev. B **87**, 054301 (2013).@
[7] H. J. Zeiger, J. Vidal, T.K. Cheng, E. P. Ippen, G. Dresselhaus and M.S. Dresselhaus, Phys. Rev. B **45**, 768 (1992).
[8] A. V. Kuznetsov and C.J. Stanton, Phys. Rev. Lett. **73**, 3243 (1994).
[9] G. A. Garrett, T. F. Albrecht, J. F. Whitaker and R. Merlin, Phys. Rev. Lett., **77**, 3661 (1996).
[10] R. Merlin, Solid State Commun. **102**, 207 (1997).
[11] T. E. Stevens, J. Kuhl, and R. Merlin, Phys. Rev. B **65**, 144304 (2002).
[12] For a new route to excitation of coherent phonons via nonlinear coupling between Raman-active mode and Infrared active mode, see M. Först, C. Manzoni, S. Kaiser, Y. Tomioka, Y. Tokura, R. Merlin, and A. Cavalleri, Nature Phys. **7**, 854 (2011).
[13] K. G. Nakamura, Y. Shikano and Y. Kayanuma, Phys. Rev. B**92**, 144304 (2015).
[14] K. Ishioka, M. Kitajima, and O. V. Misochko, J. Appl. Phys. **100**, 093501 (2006).
[15] A. A. Melnikov, O. V. Misochko, and S. V. Chekalin, Phys. Lett. A, **375**, 2017 (2011).
[16] K. Ishioka, M. Kitajima, and O. V. Misochko, J. Appl. Phys. **103**, 123505 (2008).
[17] K. Norimatsu, J. Hu, A. Goto, K. Igarashi, T. Sasagawa, and K. G. Nakamura, Solid State Commun. **157**, 58 (2013).
[18] K. Norimatsu, M. Hada, S. Yamamoto, T. Sasagawa, M. Kitajima, Y. Kayanuma, and K. G. Nakamura, J. Appl. Phys. **117**, 143102 (2015).
[19] O. V. Misochko, J. Flock, and T. Dekorsy, Phys. Rev. **91**, 174303 (2015).
[20] R. Loudon, *Quantum Theory of Light*, Oxford University Press, 3rd Edition, Oxford (2000).
[21] H. A. Jahn and E. Teller, Proc. Roy. Soc. A, **161**, 220 (1937).
[22] H. C. Longuet-Higgins, U.Öpik, M. H. L. Pryce, and R. A. Sack, Proc. Loyal Soc. London, **244**, 1 (1958).
[23] See for example, M. C. M. O'Brien and C. C. Chancey, Am. J. Phys. **61**, 688 (1993) .
[24] Y. Toyozawa and M. Inoue, J. Phys. Soc. Jpn. **21**, 1663 (1966).
[25] C. C. Yu and P. W. Anderson, Phys. Rev B **29**, 6165 (1984).
[26] A. Heinz and R. D. Tscheuschner, Phys. Rev. B **43**, 5601 (1991).
[27] H. Keller, A. Bussmann-Holder, and K. A. Müller, Mater. Today, **11**, 38 (2008).
[28] M. C. M. O'Brien, J. Phys. C **5**, 2045 (1972).
[29] Y. Kayanuma and H. Nakayama, Phys. Rev. B **57**, 13099 (1998).
[30] Note that in [11], the frequencies of photon and phonon are denoted by ω and Ω, respectively.
[31] As a preliminary report, see S. Hayashi *et al.* Sci. Rep. **4**, 4456 (2014).
[32] K. G. Nakamura *et al.*, unpublished.
[33] K. J. Yee, K. G. Lee, E. Oh, and D. S. Kim, and Y. S. Lim, Phys. Rev. Lett. **88**, 105501 (2002).
[34] I. H. Lee, K. J. Yee K. G. Lee, E. Oh, and D. S. Kim, J. Appl. Phys. **93**, 4939 (2003).

[35] D. Suzuki, H. Kunugita, and K. Ema, J. Phys. Conference Series, **193**, 012052 (2009).
[36] M. Esposito, K. Titimbo, K. Zimmermann, F. Giusti, F. Randi, D. Boschetto, F. Parmigiani, R. Floreanini, and D. Fausti, Nat. Comm. **6**, 10249 (2015).
[37] O. V. Misochko and M. V. Lebedev, Phys. Rev. B **94**, 184307 (2016).
[38] J. J. Li, J. Chen, D. A. Reis, S. Fahy, and R. Merlin, Phys. Rev. Lett. **110**, 047401 (2013).

Appendix: Calculation of dynamical factors

We derive formulas (27) and (28). As described in the text, we may concentrate on the calculation of the dynamical factors $L_A(\Omega_0)$ and $L_S(\Omega_0)$ assuming that the excited states are composed of a non-degenerate single band $|k\rangle \equiv a^\dagger_{k,e}a_{k,s}|g\rangle$ with the ground state $|g\rangle \equiv \prod_k a^\dagger_{k,s}|\mathrm{vac}\rangle$. The degeneracy of the phonon modes is also neglected as if they are fully symmetric mode. Then we have only two types Feynman diagram corresponding to IA and ISRS.

For ISRS, we calculate the ket vector $|\psi^s_u(t)\rangle$ at time $t(>>\sigma)$ corresponding to the upper propagators of Fig. 2. It is in the second order term of perturbation expansion with respect to $H_{eR}(t)$ and the first order term with H_{eL},

$$|\psi^s_u(t)\rangle = \left(\frac{-i}{\hbar}\right)^3 E^2\alpha\hbar\omega\int_{-\infty}^{t}d\tau_2\int_{-\infty}^{\tau_2}d\tau_1\int_{\tau_1}^{\tau_2}dx f(\tau_1)f(\tau_2)e^{i\Omega_0(\tau_2-\tau_1)}e^{i\omega x}F(\tau_2-\tau_1)e^{-i\omega t}b^\dagger|g\rangle, \tag{A.1}$$

where we set the energy of the ground state equal to zero. The integral over the phonon vertex x yields a factor $\left(e^{i\omega\tau_2}-e^{i\omega\tau_1}\right)/(i\omega)$. The integral over τ_1 and τ_2 is performed as follows. We introduce a new variables $s \equiv (\tau_2+\tau_1)/2$, $\quad u\equiv\tau_2-\tau_1$, and rewrite $f(\tau_1)f(\tau_2)$ as

$$f(s-\frac{u}{2})f(s+\frac{u}{2}) = \frac{1}{\pi\sigma^2\Omega_0^2}\exp\left[-(\frac{2s^2}{\sigma^2}+\frac{u^2}{2\sigma^2})\right]. \tag{A.2}$$

Because of the assumption $t>>\sigma$, the integral domain is safely extended to $-\infty<s<\infty$ and $0<u<\infty$. The Gaussian integral over s is carried out analytically, and we find

$$|\psi^s_u(t)\rangle = 2i\left(\frac{E}{\hbar\Omega_0}\right)^2\alpha\frac{1}{\sqrt{2\pi}\sigma}e^{-\sigma^2\omega^2/8}\int_0^\infty du e^{-\frac{u^2}{2\sigma^2}}\sin\left(\frac{\omega u}{2}\right)e^{i\Omega_0 u}F(u)e^{-i\omega t}b^\dagger|g\rangle. \tag{A.3}$$

The lower propagator is the unperturbed state $|\psi^s_l(t)\rangle = |g\rangle$. The expectation value of the annihilation operator b is then given by $\langle\psi^s_l(t)|b|\psi^s_u(t)\rangle$, and together with its Hermitian conjugate, we obtain $L_S(\Omega_0)$ in Eq. (28) for the expectation value of Q(t) in ISRS.

For IA, the upper propagator is calculated to the first order of $H_{eR}(t)$ and H_{eL} as

$$|\psi^a_u(t)\rangle = \left(\frac{-i}{\hbar}\right)^2 E\alpha\hbar\omega\sum_k\mu_k\int_{-\infty}^{t}d\tau_1\int_{\tau_1}^{t}dx f(\tau_1)e^{i\omega x}e^{-i(\hbar\Omega_0-\epsilon_k)\tau_1/\hbar}e^{-i(\epsilon_k+\hbar\omega)t/\hbar}b^\dagger|k\rangle. \tag{A.4}$$

The integration over x yields $\left(e^{i\omega t}-e^{i\omega\tau_1}\right)/(i\omega)$. The ket vector for the lower propergator is given by

$$|\psi^a_l(t)\rangle = -i\frac{E}{\hbar}\sum_{k'}\mu_{k'}\int_{-\infty}^{t}d\tau_2 f(\tau_2)e^{-i(\hbar\Omega_0-\epsilon_{k'})\tau_2/\hbar}e^{-i\epsilon_{k'}t}|k'\rangle. \tag{A.5}$$

The expectation value for b is now given by

$$\langle\psi^a_l(t)|b|\psi^a_u(t)\rangle = \left(\frac{E}{\hbar}\right)^2\alpha\int_{-\infty}^{t}d\tau_2\int_{-\infty}^{t}d\tau_1 f(\tau_1)f(\tau_2)\left(e^{i\omega\tau_1}e^{-i\omega t}-1\right)e^{i\Omega_0(\tau_2-\tau_1)}F(\tau_2-\tau_1). \tag{A.6}$$

Again, setting $t\to\infty$ in the upper limit of the integrals, and changing the variables from (τ_1,τ_2) to (s,u) as before, we find

$$\langle\psi^a_l(t)|b|\psi^a_u(t)\rangle = \left(\frac{E}{\hbar\Omega_0}\right)^2\alpha\frac{1}{\sqrt{2\pi}\sigma}\left\{e^{-\sigma^2\omega^2/8}\int_{-\infty}^{\infty}du e^{-\frac{u^2}{2\sigma^2}}e^{i(\Omega_0-\frac{\omega}{2})u}F(u)e^{-i\omega t}-\int_{-\infty}^{\infty}du e^{-\frac{u^2}{2\sigma^2}}e^{i\Omega_0 u}F(u)\right\}. \tag{A.7}$$

Together with the Hermitian conjugate of the above equation, we arrive at Eq.(27).